Chemical Properties of Starburst Galaxies Near and Far: Clues to Galaxy Evolution

T. Contini [1,2], M.-A. Treyer [3], M. Mouhcine [2], M. Sullivan [4], & R. S. Ellis [5]

[1] *Observatoire Midi-Pyrénées, UMR 5572, 14 avenue E. Belin, F-31400 Toulouse, France*
[2] *Observatoire de Strasbourg, 11 rue de l'Université, F-67000 Strasbourg, France*
[3] *Laboratoire d'Astrophysique de Marseille, Traverse du Siphon, F-13376 Marseille, France*
[4] *Institute of Astronomy, Madingley Road, Cambridge, CB3 OHA, UK*
[5] *California Institute of Technology, Pasadena, CA 91125, USA*

Abstract. The determination of chemical abundances in star-forming galaxies and the study of their evolution on cosmological timescales are powerful tools for understanding galaxy formation and evolution. This contribution presents the latest results in this domain. We show that detailed studies of chemical abundances in UV–selected, HII and starburst nucleus galaxies, together with the development of new chemical evolution models, put strong constraints on the evolutionary stage of these objects in terms of star formation history. Finally, we summarize our current knowledge on the chemical properties of intermediate– and high–redshift galaxies. Although the samples are still too small for statistical studies, these results give insight into the nature and evolution of distant star–forming objects and their link with present–day galaxies.

1 Introduction

Tracing the star formation history of galaxies is essential for understanding galaxy formation and evolution. The chemical properties of galaxies are closely related to their star formation history, and can be considered as fossil records, enabling us to track the galaxy formation history down to the present.

There is a lot of observational evidence suggesting that the star formation history of galaxies has not been monotonic with time, but exhibits instead significant fluctuations. Galaxies in the Local Group are excellent examples showing a variety of star formation histories. Further evidence for the "multiple-burst" scenario was recently found in massive Starburst Nucleus Galaxies (SNBGs; e.g. [6, 16]). Even the small-mass and less evolved HII galaxies seem to be formed of age-composite stellar populations indicating successive bursts of star formation (e.g. [20]).

[11] recently explored numerical models of galaxy evolution in which star formation occurs in two modes: a low-efficiency continuous mode, and a high-efficiency mode triggered by interaction with a satellite. With these assumptions, the star formation history of low-mass galaxies is characterized by intermittent bursts of star formation separated by quiescent periods lasting several Gyrs, whereas massive galaxies are perturbed on time scales of several hundred Myrs and thus have fluctuating but relatively continuous star formation histories. In these models, merger rates are specified using the predictions of hierarchical galaxy formation models (e.g. [2]).

Examining the chemical evolution and physical nature of star-forming galaxies over a range of redshifts will shed light on this issue. Emission lines from HII regions have long been the primary means of chemical diagnosis in local galaxies, but this method has only recently been applied to galaxies at cosmological distances following the advent of infrared spectrographs on 8 to 10-m class telescopes (e.g. [18, 15, 12, 1, 9, 19]) .

2 The case of UV-selected galaxies

[5] recently derived the chemical properties of a UV-selected sample of galaxies. These objects are found to be intermediate between low-mass, metal-poor HII galaxies and more massive, metal-rich SBNGs (see [6] for the dichotomy), spanning a wide range of oxygen abundances, from ~ 0.1 to 1 $Z_{\odot}$.

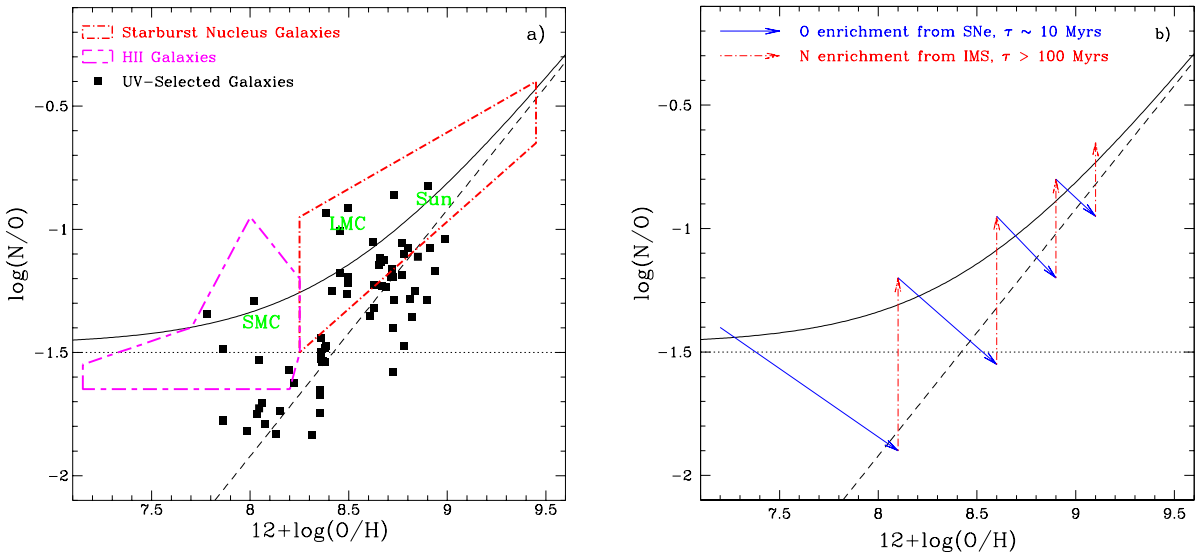

Figure 1: *a*) N/O versus $12+\log(\mathrm{O/H})$ for the UV-selected galaxies (squares; [5]) and two comparison samples of nearby star-forming galaxies: Starburst Nucleus Galaxies (dot – short dash line) selected in the optical ([4, 3]) or in the far-infrared ([21]), and HII galaxies (short dash – long dash line; [13, 10]). Theoritical curves for a *primary* (dotted line), a *secondary* (dashed line), and a *primary + secondary* (solid line) production of nitrogen ([22]) are shown. Abundances ratios for the Sun, the LMC and the SMC are also indicated. *b*) Schematic evolution model of N/O versus $12+\log(\mathrm{O/H})$ assuming a sequence of starbursts separated by quiescent periods (see also [8, 6]). This scenario assumes that each burst first produces oxygen enrichment due to massive star evolution on short time-scales ($\tau \sim 10$ Myrs), followed by significant nitrogen enrichment on longer time-scales ($\tau > 100$ Myrs) due to intermediate-mass star evolution (see [5] for details).

The behavior of these starburst galaxies in the N/O versus O/H relation (see Figure 1a) has been investigated in order to probe their physical nature and star formation history (see [5] for details). At a given metallicity, the majority of UV-selected galaxies has low N/O abundance ratios whereas SBNGs show an excess of nitrogen abundance when compared to HII regions in the disk of normal galaxies (see also [6]). The interpretation of these behaviors is not straightforward. A possible interpretation of the location of UV-selected galaxies and SBNGs in the N/O versus O/H relation could be that UV galaxies are selected at the end of a short episode of star formation following a rather long and quiescent period ([5]), whereas SBNGs experienced successive starbursts over the last Gyrs to produce the observed nitrogen abundance excess (e.g. [6])

3 Constraining the star formation history of galaxies

At a given metallicity, the distribution of N/O abundance ratios shows a large dispersion, both at low and high metallicity ([6, 5]). Only part of this scatter is due to uncertainties in the abundance determinations. The additional dispersion must therefore be accounted for by galaxy evolution models. Various hypotheses (localized chemical "pollution", IMF variations, differential mass loss, etc) were suggested as responsible for such a scatter (e.g. [14]) but none of them is able to reproduce the full N/O scatter at a given metallicity.

A natural explanation for the variation of N/O at constant metallicity might be a significant time delay between the release, into the ISM, of oxygen by massive, short-lived stars and that of nitrogen produced in low-mass longer-lived stars (see Figure 1b). The "delayed-release" model assumes that star formation is an intermittent process in galaxies, while maintaining an universal IMF and standard stellar nucleosynthesis ([7, 8]).

[17] recently investigated this possibility in order to quantifiy the star formation history of starburst galaxies. The observed dispersion in the well-known metallicity-luminosity relation has been used as an additional constraint. It was confirmed that *continuous* star formation models are unable to reproduce

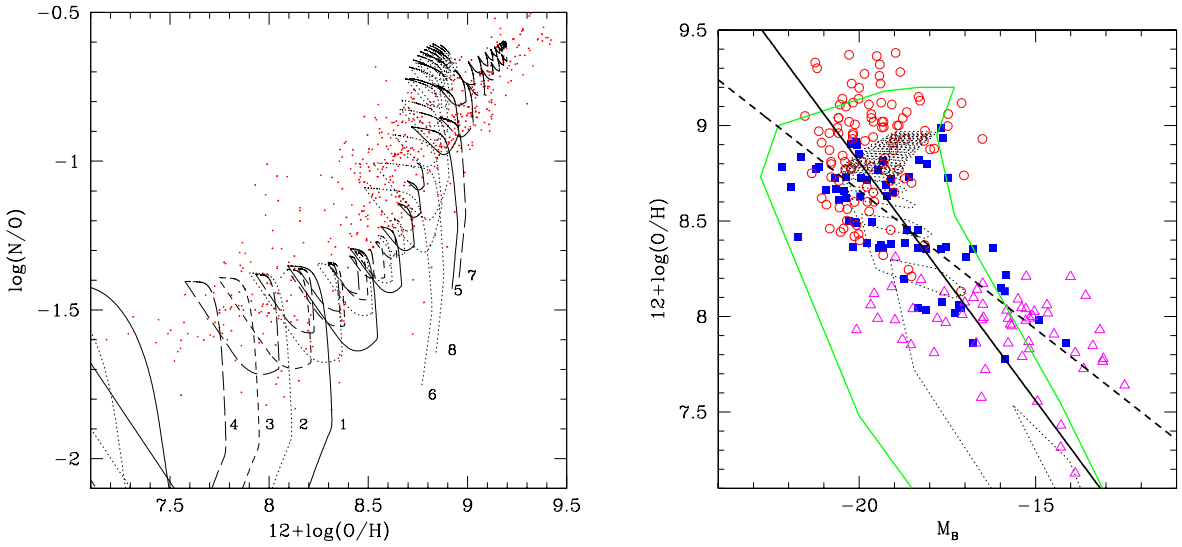

Figure 2: *Left*: N/O versus $12 + \log(\mathrm{O/H})$ for the samples of star-forming galaxies (dots) described in Figure 1. Model predictions assuming bursting star formation scenario are shown. The model parameters are listed in Table 1 of [17]. This figure shows the dichotomy between the models which reproduce the scatter in the metal-poor region ($12 + \log(\mathrm{O/H}) \leq 8.5$), and those which reproduce the scatter in the metal-rich region ($12 + \log(\mathrm{O/H}) \geq 8.5$). *Right*: The metallicity-luminosity relation for the starburst galaxy samples described in Figure 1: HII galaxies (triangles), SBNGs (circles) and UV-selected galaxies (squares). The continuous thick line is a linear fit to the whole sample of starburst galaxies, and the dashed thick line is a linear fit to local *"normal"* irregular and spiral galaxies ([15]). Model predictions assuming a bursting star formation scenario are shown. The model parameters are the same as those used in the left panel. The delineated area (thick green line) encompasses all the model predictions calculated with the parameters reported in Table 1 of [17]. For illustration, the prediction of a specific model (dotted thin line) is shown.

the scatter observed in both N/O and M_{B} versus O/H scaling relations. The dispersion associated with the distribution of N/O as a function of metallicity can indeed be explained in the framework of *bursting* star formation models. Figure 2 shows the oscillating behavior of the N/O ratio due to the alternating bursting and quiescent phases. In this case, the observed dispersion in the N/O versus O/H relation is explained by the time delay between the release of oxygen by massive stars into the ISM and that of nitrogen by intermediate-mass stars (see also Figure 1b for a schematic view). During the starburst events, as massive stars dominate the chemical enrichment, the galaxy moves towards the lower right part of the diagram. During the interburst period, when no star formation is occurring, the release of N by low and intermediate-mass stars occurs a few hundred Myrs after the end of the burst and increases N/O at constant O/H. The dilution of interstellar gas by the newly accreted intergalactic gas is also observed during the quiescent phases.

Extensive model computations (see [17] for details) show that no possible combination of the model parameters (i.e., burst duration, interburst period, star formation efficiency, gas accretion timescale, etc) is able to account for the observed spread for the whole sample of galaxies. [17] found that the most important parameter for reproducing the observed spread is the star formation efficiency. Once the star formation efficiency is set, the extent of the predicted spread mainly depends on the starburst duration. The models show that, to account for the observed scatter of N/O for the whole metallicity range, one needs to consider at least two *regimes* (low and high metallicity) characterized by different star formation efficiencies and starburst durations.

Following these models, metal-rich ($12 + \log(\mathrm{O/H}) \geq 8.5$) spiral galaxies differ from metal-poor ones by a higher star formation efficiency and starburst frequency. Moreover, the fit is very good for metal-rich galaxies if the quiescent period between two successive bursts is of the same order as the gas infall timescale. This can be understood in the context of the hierarchical galaxy formation scenario where a major burst of star formation is activated each time a galaxy undergoes a minor merger event, such as the accretion of a small satellite or primordial HI gas clouds (e.g. [2]).

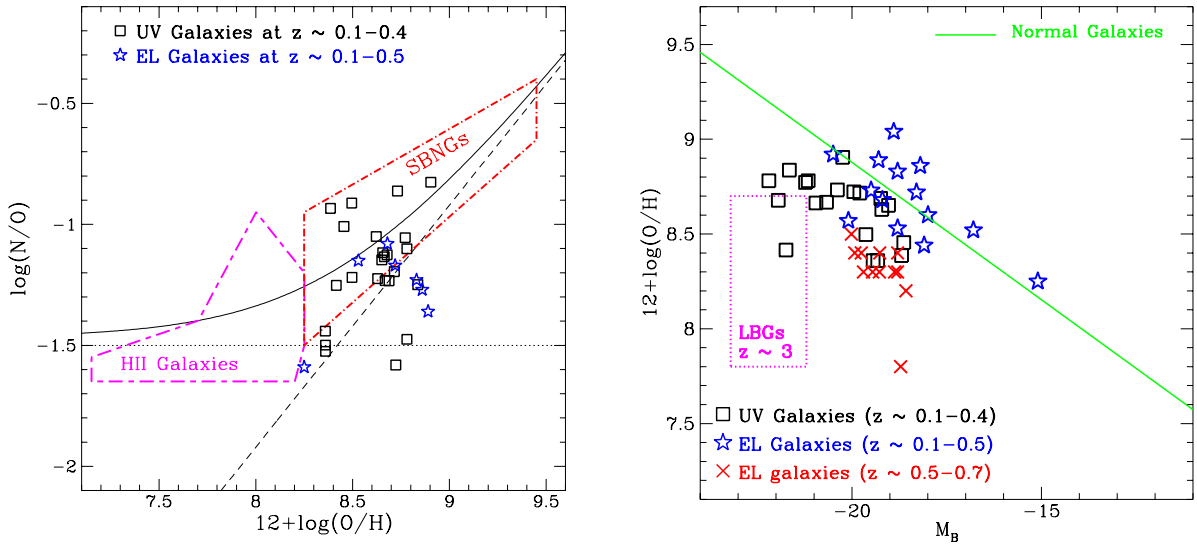

Figure 3: N/O (*left*) and absolute B-band magnitude (*right*) as a function of metallicity for intermediate and high redshift star-forming galaxies. All chemical abundance data published so far for distant galaxies are on this plot. The samples of intermediate-redshift galaxies are: UV-selected galaxies (squares; [5]) and emission-line (EL) galaxies (stars; [15]) at $z \sim 0.1 - 0.5$, compact and luminous EL galaxies at $z \sim 0.5 - 0.7$ (crosses; [9]). The location of high-redshift ($z \sim 3$) Lyman break galaxies is shown as a box encompassing the range of O/H and $M_{\rm B}$ derived for these objects ([19]). On the left panel, the location of nearby HII galaxies and SBNGs (see Figure 1 for references) is shown for comparison. The metallicity–luminosity relation for local "normal" galaxies (see [15]) is shown as a solid line on the right panel.

Finally, these models confirm previous claims ([5]) that UV-selected galaxies are observed at a special stage in their evolution. Their low N/O abundance ratios with respect to other starburst galaxies is well explained if they have just undergone a powerful starburst which enriched their ISM in oxygen.

4 Chemical properties of intermediate– and high–redshift galaxies

In Figure 3 (*left*), we compare the location of intermediate-redshift ($z \sim 0.1 - 0.4$) emission-line (EL; [15]) and UV-selected ([5]) galaxies with nearby samples of HII and SBNGs in the N/O versus O/H plane. Most of these distant objects have chemical abundances typical of massive and metal-rich SBNGs (i.e., $12 + \log({\rm O/H}) \geq 8.5$). Some of them show high N/O abundance ratios ($\log({\rm N/O}) \gtrsim -1$) which could be due to a succession of starbursts over the last few Gyrs (e.g. [6]). None of these intermediate-redshift galaxies are located in the region occupied by nearby metal-poor HII galaxies. The fact that intermediate-redshift galaxies are mostly metal-rich objects is likely to be a selection effect arising from the well-known metallicity–luminosity relationship. Only the most luminous, and thus metal-rich objects, are detected so far with the current instrumentation on 8-m class telescopes. It is interesting to note that, like a significant fraction of UV-selected galaxies, some optically-selected EL galaxies also show strikingly low N/O ratios.

The location of distant galaxies in the metallicity–luminosity relation is shown in Figure 3 (*right*). Three samples of intermediate-redshift galaxies are considered: EL galaxies at $z \sim 0.1 - 0.5$ ([15]), luminous and compact EL galaxies at $z \sim 0.5 - 0.7$ ([9]) and the UV-selected galaxies ([5]). The location of high-redshift ($z \sim 3$) Lyman break galaxies (LBGs) is shown as a box encompassing the range of O/H and $M_{\rm B}$ derived for these objects ([19]). Whereas EL galaxies with redshifts between 0.1 and 0.5 seem to follow the metallicity–luminosity relation of "normal" galaxies (solid line), there is a clear deviation for both UV-selected and luminous EL galaxies at higher redshift ($z \sim 0.5 - 0.7$). These galaxies thus appear $2 - 3$ mag brighter than "normal" galaxies of similar metallicity, as might be expected if a strong starburst had temporarily lowered their mass-to-light ratios. [9] argue that

luminous and compact EL galaxies could be the progenitors of present-day spiral bulges. The deviation is even stronger for LBGs at $z \sim 3$. Even allowing for uncertainties in the determination of O/H and $M_{\rm B}$, LBGs fall well below the metallicity–luminosity relation of "normal" local galaxies and have much lower abundances than expected from this relation given their luminosities. The most obvious interpretation ([19]) is that LBGs have mass-to-light ratios significantly lower than those of present-day "normal" galaxies.

Although the samples are still too small to derive firm conclusions on the link between distant objects and present-day galaxies, the present results give new insight into the nature and evolution of distant star-forming galaxies. No doubt that the next large-scale spectroscopic surveys on 10-m class telescopes (e.g. VIRMOS on VLT, COSMOS/EMIR on Grantecan, etc) will shed light on these fundamental issues by producing statistically significant samples of galaxies over a large range of redshifts.

Acknowledgements. We warmly thank Laurence Tresse and Marie Treyer, the organizers of this wunderbar conference together with all the people involved in the LOC (fifi, seb, henry, etc).

References

[1] Carollo C. M., Lilly S. J., 2001, ApJ, 548, L153

[2] Cole S., Lacey C. G., Baugh C. M., Frenk C. S., 2000, MNRAS, 319, 168

[3] Considère S., Coziol R., Contini T., Davoust, E., 2000, A&A, 356, 89

[4] Contini T., Considère S., Davoust E., 1998, A&AS, 130, 285

[5] Contini T., Treyer, M.-A., Sullivan M., Ellis R.S., 2001, MNRAS, in press (astro-ph/0109395)

[6] Coziol R., Reyes R. E. C., Considère S., Davoust E., Contini T., 1999, A&A, 345, 733

[7] Edmunds M. G., Pagel B. E. J., 1978, MNRAS, 185, 777

[8] Garnett D. R., 1990, ApJ, 363, 142

[9] Hammer F., Gruel N., Thuan T. X., Flores H., Infante L., 2001, ApJ, 550, 570

[10] Izotov Y. I., Thuan T. X., 1999, ApJ, 511, 639

[11] Kauffmann G., Charlot S., Balogh M. L., 2001, Apj in press (astro-ph/0103130)

[12] Kobulnicky H. A., Koo D. C., 2000, ApJ, 545, 712

[13] Kobulnicky H. A., Skillman E. D., 1996, ApJ, 471, 211

[14] Kobulnicky H. A., Skillman E. D., 1998, ApJ, 497, 601

[15] Kobulnicky H. A., Zaritsky D., 1999, ApJ, 511, 118

[16] Lançon A., Goldader J.D., Leitherer C., Delgado R.M.G., 2001, ApJ, 552, 150

[17] Mouhcine M., Contini T., 2001, A&A, submitted

[18] Pettini M., Kellogg M., Steidel C. C., et al., 1998, ApJ, 508, 539

[19] Pettini M., Shapley A. E., Steidel C. C., et al., 2001, ApJ, 554, 981

[20] Raimann D., Storchi-Bergmann T., Bica E., Melnick J., Schmitt H., 2000, MNRAS, 316, 559

[21] Veilleux S., Kim D., Sanders D. B., Mazzarella J. M., Soifer B. T., 1995, ApJS, 98, 171

[22] Vila Costas M. B., Edmunds M. G., 1993, MNRAS, 265, 199